

Biophysical Journal, Volume 98

Supporting Material

Elongational Flow Induces the Unfolding of von Willebrand Factor at Physiological Flow Rates

Charles E. Sing and Alfredo Alexander-Katz

Elongational Flow Induces the Unfolding of von Willebrand Factor at Physiological Flow Rates

Charles E. Sing*, Alfredo Alexander-Katz*

*Department of Materials Science and Engineering, Massachusetts Institute of Technology, 77 Massachusetts Ave. 12-009, Cambridge MA 02139

ABSTRACT The unfolding of von Willebrand Factor (vWF) has been shown to be a crucial step in the process of blood clotting. Here we show that elongational flows, such as those appearing during vasoconstriction or stenosis, are the primary activation mechanisms of vWF, and unfold the multimeric protein at flow rates 2 orders of magnitude below those corresponding to pure shear. This finding complements the current understanding of blood clotting from the molecular to the physiological level, and gives new insights into the connection between clotting anomalies, such as stenosis and Heyde's syndrome.

Supplementary Material

Address reprint requests and inquiries to A. Alexander-Katz, E-mail: aalexand@mit.edu

Simulation Methods

We consider the polymer to be composed of N beads of radius a interacting through a potential U . The dynamics of the i th bead position \mathbf{r}_i is given by the Langevin equation:

$$\frac{\partial}{\partial t} \mathbf{r}_i = \mathbf{v}_\infty(\mathbf{r}_i) - \sum_j \mu_{ij} \cdot \nabla_{\mathbf{r}_i} U(t) + \xi_i(t) \quad (1)$$

where $\mathbf{v}_\infty(\mathbf{r})$ is the undisturbed solvent flow profile, μ_{ij} is a mobility matrix, and ξ_i is a random velocity that satisfies $\langle \xi_i(t) \xi_j(t') \rangle = 2k_B T \mu_{ij} \delta(t - t')$. For simple elongational flow the undisturbed flow profile is $\mathbf{v}_\infty(\mathbf{r}) = \dot{\epsilon} z \hat{\mathbf{z}} - 0.5 \dot{\epsilon} x \hat{\mathbf{x}} - 0.5 \dot{\epsilon} y \hat{\mathbf{y}}$ where $\dot{\epsilon}$ is the extensional flow rate, x, y, z are the spatial coordinates, and $\hat{\mathbf{x}}, \hat{\mathbf{y}}, \hat{\mathbf{z}}$ are the unit vectors parallel to the $x, y,$ and z axis respectively. The hydrodynamic interactions with the underlying fluid are captured through the mobility matrix μ_{ij} . We include hydrodynamic interactions (HI) by using the Rotne-Prager-Yamakawa (RPY) form of μ_{ij} : [1] [2]

$$\frac{\mu_{ij}}{\mu_0} = \begin{cases} \frac{3a}{4r_{ij}} \left(\left(1 + \frac{2a^2}{3r_{ij}^2}\right) \mathbf{I} + \left(1 - \frac{2a^2}{r_{ij}^2}\right) \frac{\mathbf{r}_{ij} \mathbf{r}_{ij}}{r_{ij}^2} \right) & r_{ij} \geq 2a \\ \left(1 - \frac{9r_{ij}^2}{32a^2}\right) \mathbf{I} + \frac{3}{32} \frac{\mathbf{r}_{ij} \mathbf{r}_{ij}}{ar_{ij}} & r_{ij} \leq 2a \end{cases} \quad (2)$$

where $\mathbf{r}_{ij} = \mathbf{r}_i - \mathbf{r}_j$ is the vectorial distance between the i th and j th bead, $\mu_0 = 6\pi\eta a$ is the self-mobility of a single bead (η is the solvent viscosity), and $r_{ij} = |\mathbf{r}_{ij}|$. Notice that for $i = j$ one obtains the correct limit of the self-mobility of a single particle in unbounded flow, i.e., $\mu_{ij} = \mu_0 \mathbf{I}$. The RP tensor is an approximation to the full hydrodynamic interaction between two spheres and accounts to first order for the finite sphere size. Such hydrodynamic simulations have been successful in describing swollen polymers in various flows. [3] [4] [5]

The potential energy U is written as $U = U_S + U_{LJ}$. The term accounts for the connectivity of the chain is given

by: [6]

$$U_S = \frac{\kappa}{2} k_B T \sum_{i=1}^{N-1} (r_{i+1,i} - 2a)^2 \quad (3)$$

where $r_{i+1,i}$ is the distance between adjacent beads along the chain, and the spring constant is taken to be $\kappa = 200/a^2$ which limits stretching of the chain to a negligible level. The second term is a Lennard-Jones potential written as:

$$U_{LJ} = \tilde{u} k_B T \sum_{ij} \left((2a/r_{ij})^{12} - 2(2a/r_{ij})^6 \right) \quad (4)$$

where \tilde{u} determines the depth of the potential (in units of $k_B T$). By varying this quantity one can tune the polymer to be swollen (small \tilde{u}) or collapsed (large \tilde{u}). To simulate the dynamics of the polymer in elongational flow, we discretize eq. 1 and use a time step Δt of $10^{-4} \tau$, where τ is the characteristic monomer diffusion time $\tau = a^2 / \mu_0 k_B T$. Averages are taken over a total number of Langevin steps of at least 2×10^7 , with the first 10^6 simulation steps typically discarded for equilibration.

Elongational Flow in a Gradient Blood Vessel Radius

Here we elaborate on the presence of an elongational flow profile in the midst of a blood vessel that is changing radii. While the results here are generally applicable, we consider only the simple case of a linear radius gradient. We again present the flow profile upon entrance to a smaller vessel from a larger one that was considered in Figure 1 in Figure S1. We also reiterate that the elongational flow in this profile occurs to the greatest extent in the center of the vessel as the velocity of the fluid flow is accelerated over (roughly) the length D . The elongational nature of this flow stems from the fact that, at any given point in this regime, the velocity of the fluid preceding the point is slower than the fluid ahead

of it. From the reference frame of this point, it appears that it is "stretched" in this direction. Graphically, we can clearly represent this by subtracting out the reference velocity of a given point. In Figure S1 we specifically consider the point in the red box. This is at the maximum of the velocity gradient and is thus the point of maximum elongational flow rate. The velocity vector at this position is subtracted from the rest of the vectors in the profile, and the resulting profile

in the direct vicinity is given in Figure S2a. Figure S2b is a purely elongational flow profile (for comparison). We note that, while not a perfect match, it is apparent that both flow fields overwhelmingly contain the same features, notably the stretching portion of the flow in the z -direction. This verifies the notion that the flow given in Figure S1 is indeed an elongational flow.

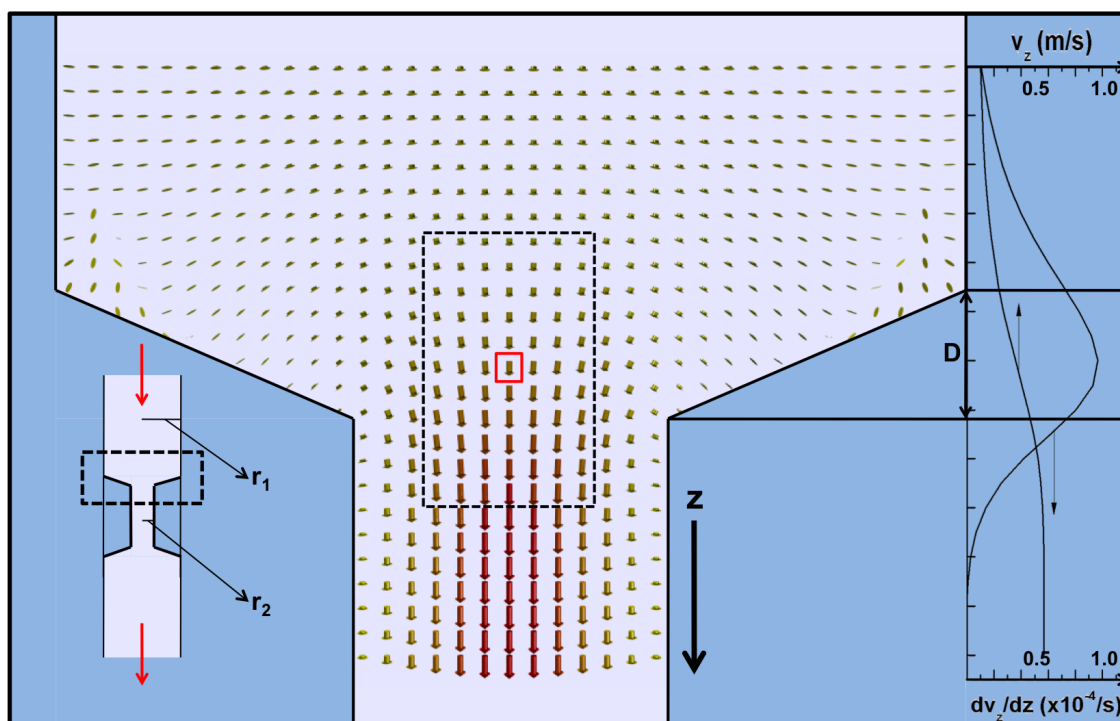


FIGURE 1 The flow profile considered in Figure 1, with the point of interest (whose velocity will now become the reference velocity) shown in a red box. This point is chosen since it occurs at a maximum velocity gradient (as seen in the graph to the right). We will look at the profile immediately surrounding this point at the points contained within the black dotted box.

REFERENCES and FOOTNOTES

1. Rotne, J. and S. Prager. 1969. Shear-induced unfolding triggers adhesion of von Willebrand Factor fibers. *J. Chem. Phys.* 50:4831.
2. H. Yamakawa. 2003. Transport properties of polymer chains in dilute solution: Hydrodynamic interaction. *J. Chem. Phys.* 53:436–443.
3. Schroeder, C.M., Shaqfeh, E.S.G., and S. Chu. 2004. Effect of hydrodynamic interactions on DNA dynamics in extensional flow: Simulation and single molecule experiment. *Macromolecules.* 37:9242–9256.
4. Jendrejack, R.M., de Pablo, J.J., and M.D. Graham. 2002. Stochastic simulations of DNA in flow: Dynamics and the effects of hydrodynamic interactions. *J. Chem. Phys.* 116:7752–7759.
5. R.G. Larson. 2005. The rheology of dilute solutions of flexible polymers: Progress and problems. *J. Rheol.* 49:1–70.
6. Alexander-Katz, A., and R.R. Netz. 2008. Dynamics and instabilities of collapsed polymers in shear flow. *Macromolecules.* 41:3363–3374.

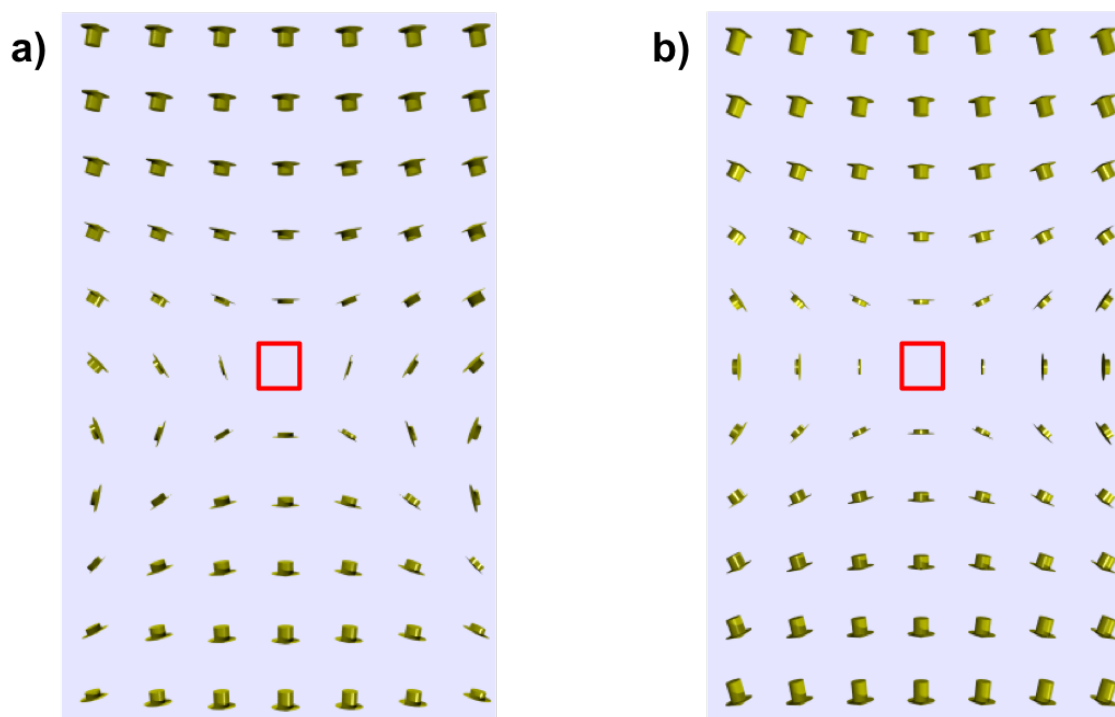


FIGURE 2 a) The area contained in the black dotted box shown above in Figure S1 with the reference velocity subtracted from every vector. b) A pure elongational flow using similar values (as described in equation 1) We note that both a) and b) are almost identical, corroborating the assertion that a change in vessel radius produces a local elongational flow.